Supplement of Atmos. Chem. Phys., 23, 8149–8168, 2023
https://doi.org/10.5194/acp-23-8149-2023-supplement

Atmospheric Chemistry and Physics
Open Access

Supplement of

Intra- and interannual changes in isoprene emission from central Amazonia

Eliane Gomes Alves et al.

Correspondence to: Eliane Gomes Alves (egomes@bgc-jena.mpg.de)

Leaf demography and phenology - phenotype description

A complete description about the installation of the Phenocam on the tower, data collection, image selection and crown selection are given in Lopes et al. (2016) and Gonçalves et al. (2020). The camera monitors 194 upper canopy trees that are free of vines, and evident and massive flush events were observed for 69% of the 194, representing 134 trees. The definition of phenotypes of the 134 trees is:

1. Evergreen: tree crowns that remain green but have detectable flushes, with at least four over the sampling period (2013-2018).
2. Semi-evergreen: similar to evergreen, but flushing maximum three times over the entire sampling period (2013-2018).
3. Brevidecidous: tree crowns that have a brief abscised stage (bare) followed by flushing, approximately every year (2013-2018).
4. semi-brevidecidous: tree crowns that have a brief abscised stage (bare) followed by flushing, but the difference with brevidecidous is that the flushing-abscission dynamics is irregular.

The left 60 tree individuals did not present evident and massive flush events, and therefore it is assumed that they flush new leaves continuously across the year (Lopes et al., 2016).

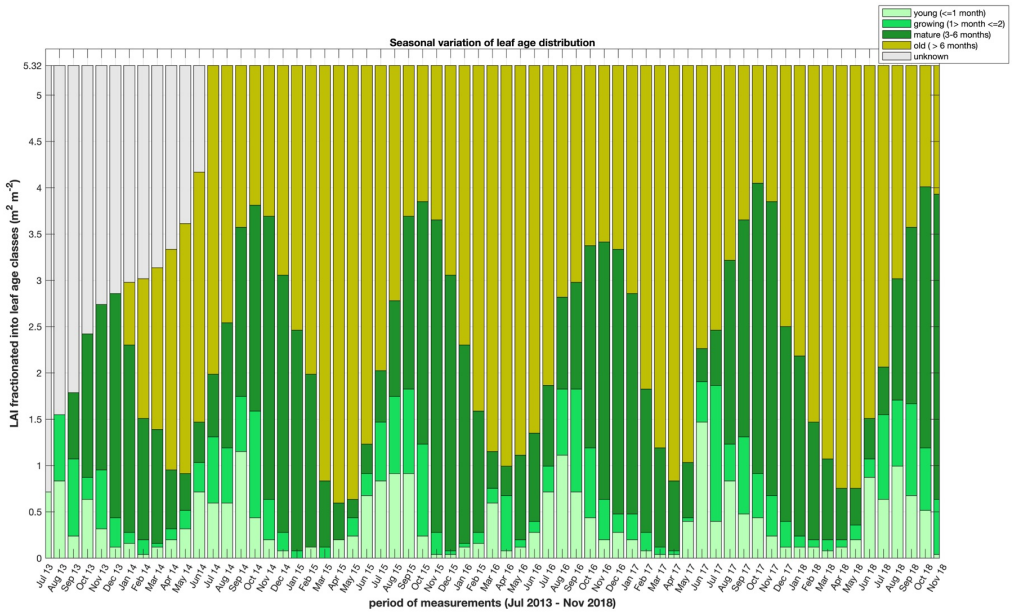

Figure S1. LAI fractionated into leaf age classes from July 2013 to November 2018.

In-canopy micrometeorology and eddy covariance flux uncertainties

To assess the within-canopy air mixing, we analyzed the 2022 datasets of all months we have field campaigns in the past (Feb, Mar, Aug, Sep, Oct, and Nov). Figure S2 shows the Bowen ratio (bottom panel), latent heat flux (middle panel), and sensible heat flux (top panel) measured at 24 m.

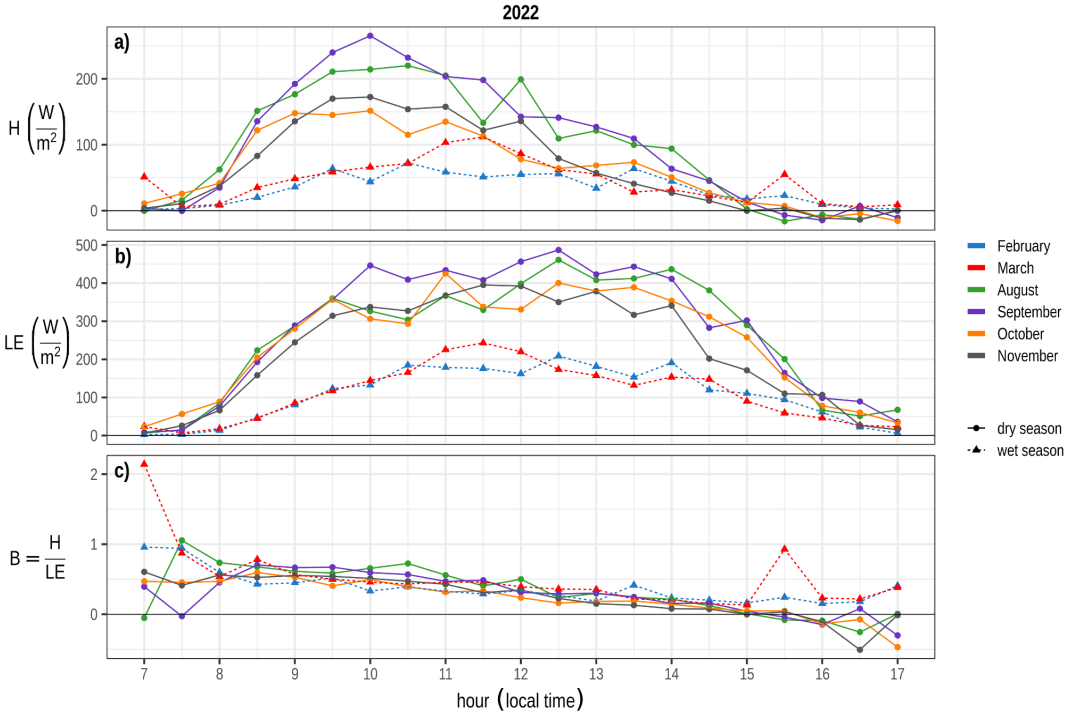

Figure S2: Diurnal cycle (07:00-17:00h, local time) of sensible (a) and latent heat (b) fluxes in Wm^{-2} using data averaged every 30 mins processed with EddyPro Software, and the Bowen ratio calculated for this period (c). Colored lines represent their respective month in 2022, and the dry season is represented by a solid line with points, whereas the dashed lines with triangles refer to the wet season.

We observed that both sensible and latent heat fluxes increased in the dry season, resulting in a very similar Bowen ratio between seasons, especially for the daytime period in which we analyzed isoprene mixing ratios (12:00-15:00, local time). We also considered another parameter that infers the in-canopy stability. For that, we analyzed the canopy profiles of the potential temperature of all months that we had campaigns in 2013, 2014, and 2015 and normalized them to the temperature measured at the top canopy (36 m), accounting for the daytime period that we analyzed isoprene mixing ratios (12:00-15:00, local time) (Figure S3).

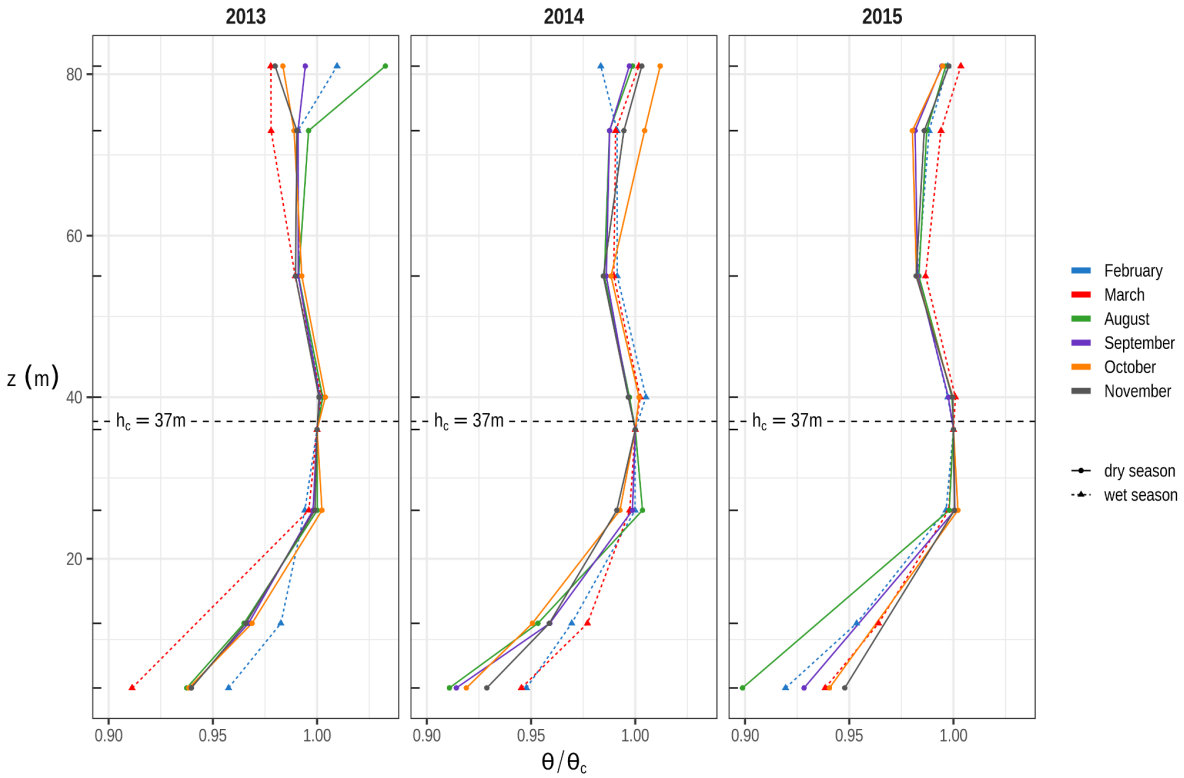

Figure S3: Mean vertical profiles of the potential temperature (Θ) in °C (12:00-15:00 local time), normalized to the potential temperature (Θ_c) measured at the mean canopy height (36 m). The heights represented are 4, 12, 26, 36, 40, 55, 73, and 81m.

We observed that for all seasons across the years, the atmosphere was stable below 24m, neutral between 24 and 40 m, and unstable above 40 m. These in-canopy stability profiles and Bowen ratio values suggest that, although air mixing might affect isoprene mixing ratio profiles, the higher isoprene concentrations in specific heights (e.g., 24 m in Nov 2012) result from higher emissions; similarly, the lower isoprene concentrations in the same specific heights, but different seasons, result from lower emissions.

Regarding the uncertainties of eddy covariance measurements, we calculated systematic and random uncertainties for the isoprene (m69) fluxes. Systematic errors lead to the failure to capture all of the largest transporting scales, typically leading to an underestimation of the flux. The random error is due to inadequate sampling of the main transporting eddies because of using too short a record length (Vickers et al., 2009). We used the method described by Finkelstein and Sims (2001) to estimate the random flux uncertainty. The integral turbulence scale (ITS) was defined as the cross-correlation first crossing 1/e with a maximum correlation period of 10 s. Mean daytime uncertainties of eddy covariance isoprene flux were at most 15%.

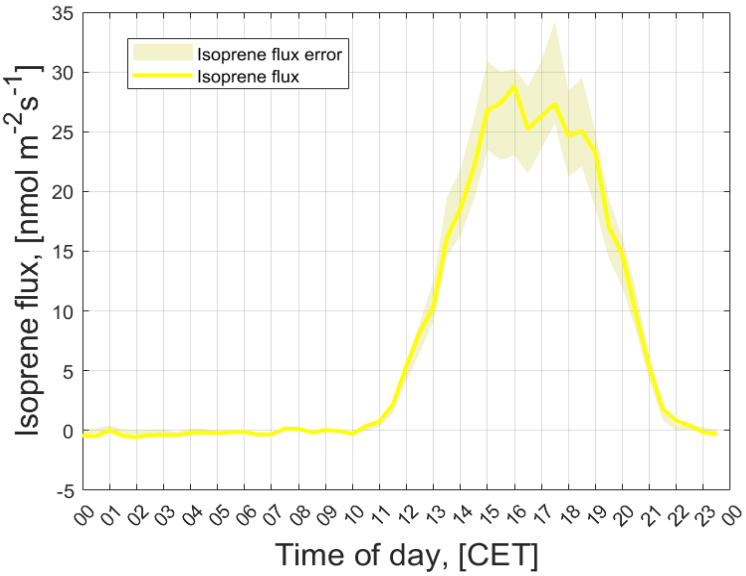

Figure S4. Mean diel variation of isoprene flux and the flux error during the period of investigation.

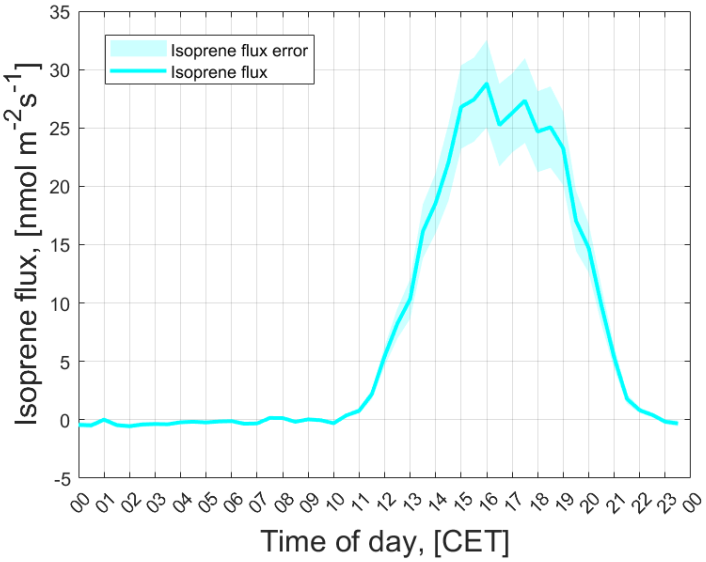

Figure S5. Median diel variation of isoprene flux and the flux error during the period of investigation.

The main sources of systematic uncertainties were sonic anemometer tilt, spatial separation between the sonic anemometer and the inlet tube, lag time between the vertical wind speed component w and the isoprene concentration due to transport time of the air sample through a long tube from the tower to the PTRMS on the ground. We corrected for these sources of uncertainty by applying the standard methods of correction (coordinate rotation, spectral correction in the high and low frequency range, and time lag correction respectively) using the eddy covariance software package Eddypro (LI-COR Biosciences, Lincoln, USA).

More details about these procedures and the data quality control can be found in Pfannerstill et al. (2018) and Pfannerstill et al. (2022).

Tables

Table S1: Isoprene emission capacity across species and leaf ages (days after flushing). Values within brackets represent one standard deviation of mean.

tree species	Isoprene (mg m^{-2} h^{-1})	leaf age (days)	leaf age class*	emitter categogy	height (m)	date of measurements
Eschweilera amazonica	2.79	61	mature	medium	23	Nov 3, 2017
Eschweilera bracteosa	2.35	59	growing	medium	24	Nov 1, 2017
Stryphnodendron racemiferum	3.52	123	mature	medium	24	Nov 3, 2017
Stryphnodendron racemiferum	3.30	425	old	medium	24	Nov 2, 2017
Protium apiculatum	2.26	121	mature	medium	24	Nov 1, 2017
Protium apiculatum	1.19	486	old	medium	24	Nov 1, 2017
Protium guianense	2.05	112	mature	medium	21	Oct 22, 2017
Protium guianense	0.83	414	old	medium	24	Oct 23, 2017
Sacoglottis cf. guianensis	1.48	112	mature	medium	24	Oct 23, 2017
Sacoglottis cf. guianensis	2.02	446	old	medium	24	Oct 23, 2017
Gustavia elliptica	0.56	116	mature	low	22	Oct 27, 2017
Gustavia elliptica	0.60	295	old	low	22	Oct 27, 2017
Helicostylis tomentosa	not detected	20	young	low	26	Oct 27, 2017
Helicostylis tomentosa	0.49	143	mature	low	26	Oct 24, 2017
Eugenia cuspifolia	0.45	107	mature	low	26	Oct 18, 2017
Eugenia cuspifolia	0.08	409	old	low	26	Oct 18, 2017
Eschweilera cyathiformis	0.30	122	mature	low	30	Nov 2, 2017
Eschweilera cyathiformis	0.03	578	old	low	30	Nov 2, 2017
Symphonia globulifera	0.13	138	mature	low	26	Oct 19, 2017
Symphonia globulifera	0.08	258	old	low	26	Oct 19, 2017
morphotype 1	0.12	79	mature	low	30	Oct 21, 2017
morphotype 1	0.07	475	old	low	30	Oct 21, 2017
Pouteria fimbriata	not detected	301	old	not detected	26	Nov 2, 2017
Mouriri cf. brevipes	not detected	414	old	not detected	26	Oct 23, 2017
Chimarrhis turbinata	not detected	110	mature	not detected	26	Oct 21, 2017

	not detected		old	not		
Chimarrhis turbinata		475		detected	26	Oct 21, 2017
			young	not		
Mouriri cf. dimorphandra	not detected	15		detected	32	Oct 19, 2017
			mature	not		
Mouriri cf. dimorphandra	not detected	108		detected	32	Oct 19, 2017
			old	not		
Mouriri cf. dimorphandra	not detected	503		detected	32	Oct 19, 2017
			mature	not		
Mouriri cf .duckeana	not detected	82		detected	24	Oct 24, 2017
			old	not		
Mouriri cf .duckeana	not detected	415		detected	24	Oct 24, 2017
			young	not		
Apeiba glabra	not detected	17		detected	26	Oct 21, 2017
			mature	not		
Aspidosperma sandwithianum	not detected	123		detected	23	Nov 3, 2017
			young	not		
Geissospermum argenteum	not detected	23		detected	22	Oct 27, 2017
			old	not		
Geissospermum argenteum	not detected	358		detected	22	Oct 27, 2017
*Hymenaea courbaril***	0.06	0	young	high		Sep 24, 1999
*Hymenaea courbaril***	0.54	10	young	high		Oct 04, 1999
*Hymenaea courbaril***	0.68	11	young	high		Oct 05, 1999
*Hymenaea courbaril***	2.06	13	young	high		Oct 07, 1999
*Hymenaea courbaril***	11.17	28	young	high		Oct 22, 1999
*Hymenaea courbaril***	9.12	29	young	high		Oct 23, 1999
*Hymenaea courbaril***	5.60	226	old	high		May 08, 1999
*Hymenaea courbaril***	6.71	227	old	high		May 09, 1999

* leaf age classes: young leaves (0−1 month), growing (1−2 months), mature leaves (3−6 months), and old leaves (>6 months)

** Fauset et al. (2015)

***Measurements from the Southwestern Amazonia (Kuhn et al., 2004b)

Table S2: Tree species monitored with the phenocam installed on the INSTANT tower and the isoprene emission trait.
File: .xlsx

Table S3: Isoprene emission trait source. The isoprene emission trait was attributed according to literature, new measurements and imputed as in Taylor et al. (2018, 2019).
File: .xlsx